TDOA/AOD/AOA LOCALIZATION IN NLOS ENVIRONMENTS

Behailu Y. Shikur and Tobias Weber

Institute of Communications Engineering, University of Rostock, 18119 Rostock, Germany
Email: {behailu.shikur, tobias.weber}@uni-rostock.de

ABSTRACT

In this paper we present a novel localization algorithm for use in non-line-of-sight environments. We use the single bounce scattering model to model the non-line-of-sight propagations and estimate the position of a mobile station when the observations are the time-difference-of-arrival, the angle-of-departure, and the angle-of-arrival. The proposed algorithm uses the geometry of the radio propagation paths to estimate the position of the mobile station. An iterative localization algorithm based on the linearization of the observation function using a first order Taylor series is also discussed. The lower bound of the variance of an unbiased mobile station position estimator is determined using the Cramer-Rao lower bound. The performance of the proposed algorithm is analyzed using measurements from a real world indoor localization scenario and using Monte-Carlo simulations. It is shown that the proposed algorithms yield a satisfactory performance.

***Index Terms*—** TDOA localization, NLOS, multipath environment, single bounce scattering

1. INTRODUCTION

Localization in terrestrial mobile radio systems is in general a challenging task. This is due to the fact that the signals in general do not propagate directly from the transmitter to the receiver. The signals are usually reflected, diffracted, absorbed or scattered by multiple obstacles, referred to as scatterers, between the transmitter and the receiver. This results in a multipath propagation. Classical localization techniques which work under the assumption of a line-of-sight (LOS) propagation often result in a very poor performance due to the non-line-of-sight (NLOS) propagations. Thus new localization algorithms which account for the NLOS propagations have to be developed. There are two major approaches for localization in NLOS environments. They are the statistical and the parametric approach. The statistical approach is rather simple and assumes that the NLOS propagations result in a positive bias to the measured time-of-arrival (TOA) of the signals. Different approaches have been investigated to identify and mitigate the NLOS bias in the measurements [1]. The parametric approach, on the other hand, models the NLOS propagation under the explicit consideration of the scatterers [2, 3, 4, 5, 6]. In this paper, we employ the single bounce scattering model, which is a simplified parametric model, and develop an algorithm to estimate the position of a mobile station (MS) in an NLOS localization scenario when the observations are the time-difference-of-arrival (TDOA), the angle-of-departure (AOD) and the angle-of-arrival (AOA). The AOD and the AOA refer to the angle of arrival at the base station (BS) and at the MS, respectively. The TDOA, the AOD, and the AOA can be estimated using, e.g., the SAGE algorithm [7] by using antenna arrays at the BS and the MS.

TDOA/AOD/AOA-based NLOS MS positioning and tracking algorithms have not been adequately researched so far. TDOA observations can be used in cases when the clock of the MS is not synchronized to the BSs. In [8] a TDOA/AOD/AOA-based NLOS MS localization algorithm has been presented. An iterative algorithm based on the linearization of the observation function using a first order Taylor series has been used to estimate the MS position. However, the convergence rate of the proposed localization algorithm is very low due to randomly generated initial guess. Besides, the accuracy of the proposed algorithm is very sensitive to the observation noise. In this paper, a novel TDOA/AOD/AOA-based NLOS MS localization algorithm is presented which uses the geometry of the radio propagation paths to estimate the MS position. A closed form expression which estimates the position of the MS is derived. An iterative algorithm using a linearization by the first order Taylor series, which uses the initial MS position estimates from the above proposed algorithm, is also presented. The Cramer-Rao lower bound is also derived to assess the performance of the proposed methods. The performance of the proposed method is also investigated using measurements from a real world indoor localization scenario.

The present paper is organized as follows. In Section 2 the system model of the NLOS MS localization is discussed. The proposed localization algorithm and the Cramer-Rao lower bound are presented in Section 3. The results of laboratory experiments and Monte Carlo simulations are discussed in Section 4. Finally, a conclusion of this paper is drawn in Section 5.

2. SYSTEM MODEL

2.1. Single bounce scattering model

As discussed in Section 1 the single bounce scattering model is used to model the NLOS propagations. In the single bounce scattering model the first few arriving signals are assumed to have propagated from the transmitter to a receiver after bouncing from a scatterer only once [9]. It must be noted that the single scatterer is an effective scatterer which represents the effect of a cluster of scatterers or one large scatterer within an area [10]. Signals from multiple bounce scattering arriving at the MS are safely neglected as they usually have small signal power due to the severe attenuation caused by the multiple scattering. The two step proximity detection algorithm presented in [4] can be applied to detect and discard multiple bounce scattering in practice. It shall be noted that the single bounce scattering model includes LOS propagation as a special case if the virtual scatterer lies on the line connecting the two nodes and the signal passes just through the virtual scatterer.

Here we consider several BSs of known positions whereas the positions of the scatterers and the position of the MS are unknown.

The authors are indebted to the German Research Foundation for funding this work under the research grant No. WE2825/5-1.

978-1-4799-2893-4/14/$31.00 ©2014 IEEE

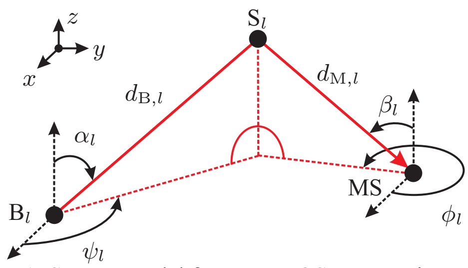

Fig. 1: System model for one NLOS propagation path

It is assumed that the MS has an unsynchronized clock and hence it is not possible to measure the NLOS propagation TOA. However, the BSs shall be synchronized with each other. Thus the MS measures the TDOA of the signals from the different BSs. For simplicity, we consider a single scatterer for each BS in the following. Thus we have a BS and scatterer pairing which is denoted by subscript l, $l \in \{1, 2, \dots, L\}$. However, in reality there are a multitude of scatterers which connect each BS to the MS. The proposed algorithm can easily be generalized to the case where several scatterers need to be considered by simply assigning more scatterers to the BSs.

Fig. 1 shows a three-dimensional (3D) system model of a single bounce scattering scenario. For simplicity only the l-th BS located at $(x_{\mathrm{B},l}, y_{\mathrm{B},l}, z_{\mathrm{B},l})$, the l-th scatterer located at $(x_{\mathrm{S},l}, y_{\mathrm{S},l}, z_{\mathrm{S},l})$ and the MS located at $(x_{\mathrm{M}}, y_{\mathrm{M}}, z_{\mathrm{M}})$ are shown. The l-th BS and scatterer are denoted by B_l and S_l, respectively. The NLOS propagation between the l-th BS and the MS is established via the l-th scatterer.

The path length d_l, the path length difference δ_l, the azimuth and elevation AOD ψ_l and α_l, and the azimuth and elevation AOA ϕ_l and β_l are calculated as follows:

$$d_{\mathrm{B},l} = \sqrt{(x_{\mathrm{S},l} - x_{\mathrm{B},l})^2 + (y_{\mathrm{S},l} - y_{\mathrm{B},l})^2 + (z_{\mathrm{S},l} - z_{\mathrm{B},l})^2}, \quad (1)$$

$$d_{\mathrm{M},l} = \sqrt{(x_{\mathrm{S},l} - x_{\mathrm{M}})^2 + (y_{\mathrm{S},l} - y_{\mathrm{M}})^2 + (z_{\mathrm{S},l} - z_{\mathrm{M}})^2}, \quad (2)$$

$$d_l = d_{\mathrm{B},l} + d_{\mathrm{M},l}, \quad (3)$$

$$\delta_l = d_l - d_1, \quad (4)$$

$$\psi_l = \frac{\pi}{2}(1 - \mathrm{sgn}(x_{\mathrm{S},l} - x_{\mathrm{B},l})) + \tan^{-1}\frac{y_{\mathrm{S},l} - y_{\mathrm{B},l}}{x_{\mathrm{S},l} - x_{\mathrm{B},l}}, \quad (5)$$

$$\phi_l = \frac{\pi}{2}(1 - \mathrm{sgn}(x_{\mathrm{S},l} - x_{\mathrm{M}})) + \tan^{-1}\frac{y_{\mathrm{S},l} - y_{\mathrm{M}}}{x_{\mathrm{S},l} - x_{\mathrm{M}}}, \quad (6)$$

$$\alpha_l = \frac{\pi}{2} - \tan^{-1}\frac{z_{\mathrm{S},l} - z_{\mathrm{B},l}}{\sqrt{(x_{\mathrm{S},l} - x_{\mathrm{B},l})^2 + (y_{\mathrm{S},l} - y_{\mathrm{B},l})^2}}, \quad (7)$$

$$\beta_l = \frac{\pi}{2} - \tan^{-1}\frac{z_{\mathrm{S},l} - z_{\mathrm{M}}}{\sqrt{(x_{\mathrm{S},l} - x_{\mathrm{M}})^2 + (y_{\mathrm{S},l} - y_{\mathrm{M}})^2}}. \quad (8)$$

The state vector $\boldsymbol{\theta}$ contains the coordinates of the MS and the scatterers in the localization scenario.

2.2. Observation model

The observations are assumed to be noisy estimates of the path length difference, the AOD, and the AOA. The observation vector function $\mathbf{h}(\boldsymbol{\theta})$ yields the path length differences, the AODs, and the AOAs of the considered paths. The noisy observation vector $\mathbf{z}$ is defined as

$$\mathbf{z} = \mathbf{h}(\boldsymbol{\theta}) + \mathbf{w}, \quad (9)$$

where $\mathbf{w}$ is the observation noise which for simplicity is assumed to be uncorrelated multivariate Gaussian distributed

$$\mathbf{w} \sim \mathcal{N}(\mathbf{0}, \mathbf{R}_{\mathrm{ww}}). \quad (10)$$

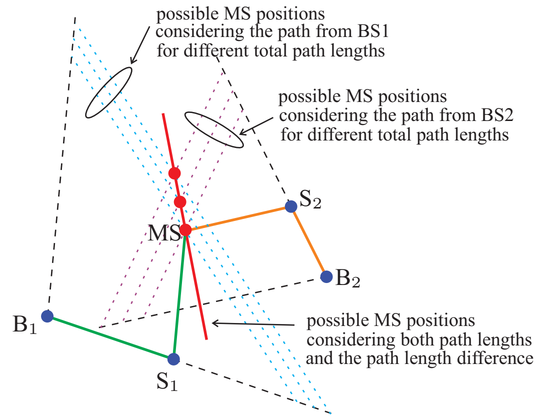

Fig. 2: 2D localization scenario for two BSs and corresponding two scatterers

Although the effective range of the AOD and the AOA is $[0, 2\pi)$, the Gaussian assumption is reasonable as shown in [11] where the estimation error of the MUSIC algorithm was shown to be asymptotically multivariate Gaussian distributed with zero mean for sufficiently large numbers of measurements.

3. ALGORITHM DERIVATION AND THE CRAMER-RAO LOWER BOUND

3.1. Localizing principle

Fig. 2 shows a localization scenario containing two BSs and two scatterers. A two-dimensional (2D) localization scenario is considered here for easier illustration of the localization process. From the AOD observations, we can draw the line on which the scatterer is located. However, since we have only the path length difference observations, the possible MS position considering a single path only spans an infinite area in the localization plane. For easier visualization, the possible MS positions for different possible path length observations are drawn as a group of parallel lines for each BS and corresponding scatterer as shown in Fig. 2. Now, considering the path length difference observation, pairs of these lines belonging to two different paths intersect at a point which is defined by the path length difference. Consideration of all the possible intersection points results in a line on which the MS is located. If we consider a third BS and a third scatterer, we can get another line on which the MS is located. The intersection point of these two lines on which the MS is located is then the estimated position of the MS. Thus it is possible to determine the MS position by considering three BSs with one corresponding scatterer each. Extension of the localization process to a 3D localization scenario is straightforward.

3.2. Formulation of the geometric algorithm

In this section we present the mathematical formulation of the localization principle discussed in Section 3.1. From Fig. 1 the position of the scatterers and the MS can be calculated as

$$x_{\mathrm{S},l} = x_{\mathrm{B},l} + d_{\mathrm{B},l}\sin\alpha_l\cos\psi_l, \quad (11)$$

$$y_{\mathrm{S},l} = y_{\mathrm{B},l} + d_{\mathrm{B},l}\sin\alpha_l\sin\psi_l, \quad (12)$$

$$z_{\mathrm{S},l} = z_{\mathrm{B},l} + d_{\mathrm{B},l}\cos\alpha_l, \quad (13)$$

$$\begin{aligned} x_{\mathrm{M}} &= x_{\mathrm{S},l} - (d_l - d_{\mathrm{B},l})\sin\beta_l\cos\phi_l \\ &= x_{\mathrm{B},l} + d_{\mathrm{B},l}a_{l,1} - (d_1 + \delta_l)\sin\beta_l\cos\phi_l, \quad (14) \end{aligned}$$

$$
\begin{aligned}
y_\mathrm{M} &= y_{\mathrm{S},l} - (d_l - d_{\mathrm{B},l})\sin\beta_l \sin\phi_l \\
&= y_{\mathrm{B},l} + d_{\mathrm{B},l} a_{l,2} - (d_1 + \delta_l)\sin\beta_l \sin\phi_l, \quad (15)\\
z_\mathrm{M} &= z_{\mathrm{S},l} - (d_l - d_{\mathrm{B},l})\cos\beta_l \\
&= z_{\mathrm{B},l} + d_{\mathrm{B},l} a_{l,3} - (d_1 + \delta_l)\cos\beta_l, \quad (16)
\end{aligned}
$$

where

$$
\begin{aligned}
a_{l,1} &= \sin\alpha_l \cos\psi_l + \sin\beta_l \cos\phi_l, \quad (17)\\
a_{l,2} &= \sin\alpha_l \sin\psi_l + \sin\beta_l \sin\phi_l, \quad (18)\\
a_{l,3} &= \cos\alpha_l + \cos\beta_l. \quad (19)
\end{aligned}
$$

Finding the expression for $d_{\mathrm{B},l}$ from (14) results in

$$
d_{\mathrm{B},l} = \frac{x_\mathrm{M} - x_{\mathrm{B},l} + (d_1 + \delta_l)\sin\beta_l \cos\phi_l}{a_{l,1}}. \quad (20)
$$

Using (20) to substitute $d_{\mathrm{B},l}$ in (15) and (16), we get

$$
-x_\mathrm{M} a_{l,2} + y_\mathrm{M} a_{l,1} = -x_{\mathrm{B},l} a_{l,2} + y_{\mathrm{B},l} a_{l,1} + (d_1 + \delta_l) a_{l,4}, \quad (21)
$$

$$
-x_\mathrm{M} a_{l,3} + z_\mathrm{M} a_{l,1} = -x_{\mathrm{B},l} a_{l,3} + z_{\mathrm{B},l} a_{l,1} + (d_1 + \delta_l) a_{l,5}, \quad (22)
$$

where

$$
\begin{aligned}
a_{l,4} &= \sin\beta_l \sin\alpha_l \sin\psi_l - \phi_l, \quad (23)\\
a_{l,5} &= \sin\beta_l \cos\phi_l \cos\alpha_l - \cos\beta_l \sin\alpha_l \cos\psi_l. \quad (24)
\end{aligned}
$$

Generating similar equations for each of the BSs and the scatterers, a matrix $\mathbf{A}$ can be defined as follows

$$
\mathbf{A} = (\mathbf{a}_1, \mathbf{a}_2, \dots, \mathbf{a}_{2L})^\mathrm{T}, \quad (25)
$$

where

$$
\begin{aligned}
\mathbf{a}_{2l-1} &= (-a_{l,2}, a_{l,1}, 0, -a_{l,4})^\mathrm{T}, \quad (26)\\
\mathbf{a}_{2l} &= (-a_{l,3}, 0, a_{l,1}, -a_{l,5})^\mathrm{T}. \quad (27)
\end{aligned}
$$

Let us denote the unknowns by the quadruple

$$
\mathbf{r} = (x_\mathrm{M}, y_\mathrm{M}, z_\mathrm{M}, d_1)^\mathrm{T}, \quad (28)
$$

where d_1 is a nuisance parameter here. The vector

$$
\mathbf{b} = (b_1, b_2, \dots, b_{2L})^\mathrm{T}, \quad (29)
$$

denotes the knowns and it is defined as

$$
\begin{aligned}
b_{2l-1} &= -x_{\mathrm{B},l} a_{l,2} + y_{\mathrm{B},l} a_{l,1} + \delta_l a_{l,4}, \quad (30)\\
b_{2l} &= -x_{\mathrm{B},l} a_{l,3} + z_{\mathrm{B},l} a_{l,1} + \delta_l a_{l,5}. \quad (31)
\end{aligned}
$$

A system of linear equations can be constructed from (21) and (22) using $\mathbf{A}$, $\mathbf{r}$ and $\mathbf{b}$ as

$$
\mathbf{A}\mathbf{r} = \mathbf{b}. \quad (32)
$$

Due to the noisy estimates of the path length difference, the AOD and the AOA, the position of the MS is estimated based on the noisy versions of the matrix $\mathbf{A}$ and the vector $\mathbf{b}$ which are denoted by $\tilde{\mathbf{A}}$ and $\tilde{\mathbf{b}}$, respectively. Assuming that we have an over-determined system of linear equations, the estimated MS position vector $\hat{\mathbf{r}}$ which minimizes the squared Euclidean distance

$$
\|\tilde{\mathbf{b}} - \tilde{\mathbf{A}}\mathbf{r}\|, \quad (33)
$$

is determined using the pseudo-inverse of the matrix $\tilde{\mathbf{A}}$ as

$$
\hat{\mathbf{r}} = \left(\tilde{\mathbf{A}}^\mathrm{T}\tilde{\mathbf{A}}\right)^{-1}\tilde{\mathbf{A}}^\mathrm{T}\tilde{\mathbf{b}}. \quad (34)
$$

Thus using (34) we can estimate the position of the MS based on the geometry of the localization scenario. We refer to this as the geometric algorithm.

3.3. Linearized least squares

Let $\mathrm{p}(\mathbf{z}|\boldsymbol{\theta})$ denote the conditional probability density function (pdf) of the observation vector $\mathbf{z}$ given the state vector $\boldsymbol{\theta}$. The maximum likelihood (ML) estimator $\hat{\boldsymbol{\theta}}$ is then given by

$$
\hat{\boldsymbol{\theta}} = \arg\max_{\boldsymbol{\theta}} \mathrm{p}(\mathbf{z}|\boldsymbol{\theta}). \quad (35)
$$

Equation (35) is a nonlinear and nonconvex maximization problem and it is difficult to find a closed-form solution. Iterative algorithms can be used which solve (35) approximately given a good initial iteration point. We thus consider the linearized least squares (LLS) algorithm which works by linearizing $\mathbf{h}(\boldsymbol{\theta})$ using a first order Taylor series and computing the weighted least squares solution iteratively [12]. The state vector $\hat{\boldsymbol{\theta}}_{n+1}$ which maximizes (35), when the linear approximation of $\mathbf{h}(\boldsymbol{\theta})$ at $\hat{\boldsymbol{\theta}}_n$ is used, is calculated as [12]

$$
\hat{\boldsymbol{\theta}}_{n+1} = \hat{\boldsymbol{\theta}}_n + \left(\mathbf{H}_n^\mathrm{T}\mathbf{R}_\mathrm{ww}^{-1}\mathbf{H}_n\right)^{-1}\mathbf{H}_n^\mathrm{T}\mathbf{R}_\mathrm{ww}^{-1}(\mathbf{z} - \mathbf{h}(\hat{\boldsymbol{\theta}}_n)), \quad (36)
$$

where $\mathbf{H}_n$ is the Jacobian matrix

$$
\mathbf{H} = \frac{\partial\mathbf{h}(\boldsymbol{\theta})}{\partial\boldsymbol{\theta}} \quad (37)
$$

evaluated at $\hat{\boldsymbol{\theta}}_n$. The LLS algorithm evaluates (36) iteratively until a desired accuracy or a maximum number of iterations are reached. The result of the geometric algorithm is used as an initial estimate. If the LLS algorithm does not converge, the result of the geometric algorithm will be used as the estimated MS position of the LLS algorithm. The LLS algorithm is said to not converge if $\|\hat{\boldsymbol{\theta}}_{n+1} - \hat{\boldsymbol{\theta}}_n\|$ is greater than a predetermined threshold.

3.4. Cramer-Rao Lower Bound (CRLB)

The CRLB determines the lower bound of the covariance matrix of an unbiased estimator $\hat{\boldsymbol{\theta}}$ [13]. The CRLB is:

$$
\xi = (\mathbf{H}^\mathrm{T}\mathbf{R}_\mathrm{ww}^{-1}\mathbf{H})^{-1}, \quad (38)
$$

where $\mathbf{H}$ is the Jacobian matrix $\mathbf{H}$ defined in (37) evaluated at $\boldsymbol{\theta}$. Even though the proposed estimators are biased, the CRLB is still used as a performance bound. Simulation results have shown that the estimation bias of the proposed algorithms is negligibly small for the considered noise variances.

4. SIMULATION AND LABORATORY RESULTS

4.1. Simulation results

Let's consider localization in a microcell scenario. The MS is assumed to be positioned at $(18, 24, 26)$ m. The positions of the four BSs are $(0, 0, 0)$ m, $(11, 40, 9)$ m, $(40, 20, 17)$ m, $(15, 28, 23)$ m and the positions of the corresponding scatterers are $(11, 27, 19)$ m, $(35, 25, 30)$ m, $(37, 17, 23)$ m, $(12, 23, 33)$ m. The standard deviation of the observation noise for the path length difference and the AOD and the AOA are denoted by σ_δ, and σ_ang, respectively. Monte-Carlo simulations have been carried out using 10^5 independent trials. The performance criterion is the root mean square error

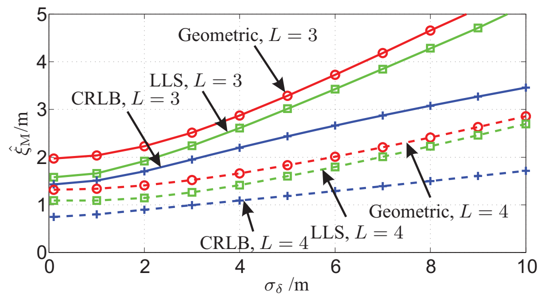

Fig. 3: RMSE of the geometric algorithm and the LLS algorithm and the CRLB versus σ_δ, $\sigma_{\mathrm{ang}} = 3°$

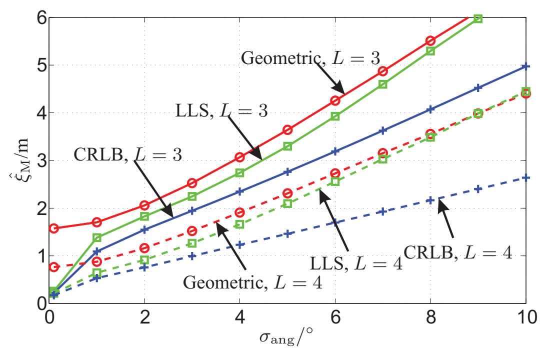

Fig. 4: RMSE of the geometric algorithm and the LLS algorithm and the CRLB versus σ_{ang}, $\sigma_\delta = 3$ m

of the MS position estimation $\hat{\xi}_{\mathrm{M}}$ which is calculated as

$$\hat{\xi}_{\mathrm{M}} = \sqrt{\frac{\mathrm{E}\{(\hat{x}_{\mathrm{M}} - x_{\mathrm{M}})^2\} + \mathrm{E}\{(\hat{y}_{\mathrm{M}} - y_{\mathrm{M}})^2\} + \mathrm{E}\{(\hat{z}_{\mathrm{M}} - z_{\mathrm{M}})^2\}}{3}}. \tag{39}$$

Fig. 3 shows the performance comparison of the geometric algorithm and the LLS algorithm for different σ_δ when $\sigma_{\mathrm{ang}} = 3°$. The CRLB of the MS position estimation is also shown. The LLS algorithm shows an improved performance compared to the geometric algorithm. The performance curve of both the geometric algorithm and the LLS algorithm are above the CRLB. Fig. 4 shows the performance of the geometric algorithm and the LLS algorithm for different σ_{ang} when $\sigma_\delta = 3$ m. It can be seen that the performance curve of the proposed algorithms is above the CRLB. At low σ_{ang} the LLS algorithm shows a significant performance improvement over the geometric algorithm and it is close to the CRLB. However, at high σ_{ang} there is little or no performance improvement by the LLS algorithm over the geometric algorithm. The LLS algorithm exhibits good convergence due to the good initial guess from the geometric algorithm. Initializing the LLS algorithm with a randomly generated value as in [8] would result in a severe performance degradation. In both Fig. 3 and Fig. 4 it can be seen that consideration of more scatterers results in a significant performance improvement.

4.2. Laboratory results

Here, we assess the performance of the geometric algorithm using real world measurements in an indoor scenario. The measurements have been performed in the microwave laboratory of the Institute of Communications Engineering at the University of Rostock. The panorama view from the MS towards the BS is shown in Fig. 5. We have considered a single BS and a single MS. The BS is located at the origin whereas the MS is located at $(-464, 6, 0)$ cm. The clock at the BS and the MS are assumed to be not synchronized and hence only TDOA observations are possible. Both the BS and the MS utilize a virtual antenna array of 36 antennas to mimic a multi-antenna station. The virtual uniform circular antenna array of radius 25 cm is implemented using a single antenna on a rotating turn table. The distance between two adjacent antenna positions is less than one half of the wavelength. The carrier frequency of the transmitted signals is 2.45 GHz and their bandwidth is 100 MHz. The channel transfer functions (CTFs) of the radio channels between the BS and the MS are measured using a vector network analyzer. The SAGE algorithm [7] is applied to the measured CTFs to estimate the physical propagation path parameters, i.e., the TDOA, the AOD and the AOA. Table 1 shows the physical propagation path parameters obtained from the SAGE algorithm for five selected NLOS propagation paths.

Fig. 5: Panorama view from the MS towards the BS

Table 1: The estimated path parameters

NLOS path, l	ψ_l	α_l	ϕ_l	β_l	δ_l /cm
1	157.1°	78.3°	29.2°	73.4°	0
2	146.3°	77.2°	38.3°	75.1°	46.9
3	178.5°	74.8°	1.3°	70.7°	-43.3
4	-153.9°	75.8°	-27.4°	74.3°	9.4
5	-173.3°	73.6°	7.1°	73.1°	-46.2

The geometric algorithm is applied to estimate the MS position from the estimated physical propagation parameters shown in Table 1. The estimated MS position and the root square error (RSE) of the geometric algorithm are shown in Table 2. It can be observed that we can get a good performance from the geometric algorithm. In accordance with the simulation results, increasing the number of considered NLOS propagation paths significantly improves the performance of the MS position estimation.

Table 2: The estimated MS positions and the corresponding RSE

NLOS paths	Estimated MS position /cm	RSE /cm
$L = 3$	$(-389.2, -52.1, -33.1)$	57.9
$L = 4$	$(-391.4, 38.8, 17.3)$	47.1
$L = 5$	$(-410.0, 30.9, 5.3)$	34.5

5. CONCLUSION

We have presented a practical localization algorithm to estimate the position of an MS in an NLOS environment based on the TDOA, the AOD and the AOA observations. The performance of the geometric algorithm has been assessed using real world laboratory measurements and by the help of Monte Carlo simulations. It has been shown that the geometric algorithm results in a satisfactory performance. The proposed iterative algorithm significantly improves the estimates of the MS position.

6. REFERENCES

[1] I. Güvenç and C.C. Chong, "A survey on TOA based wireless localization and NLOS mitigation techniques," *IEEE Communications Surveys Tutorials*, vol. 11, no. 3, pp. 107–124, 2009.

[2] N. J. Thomas, D. G. M. Cruickshank, and D. I. Laurenson, "Calculation of mobile location using scatterer information," *IEE Electronics Letters*, vol. 37, no. 19, pp. 1193–1194, Sept. 2001.

[3] H. Miao, K. Yu, and M. J. Juntti, "Positioning for NLOS propagation: Algorithm derivations and Cramer-Rao bounds," *IEEE Transactions on Vehicular Technology*, vol. 56, no. 5, pp. 2568–2580, Sept. 2007.

[4] C. K. Seow and S. Y. Tan, "Non-line-of-sight localization in multipath environments," *IEEE Transactions on Mobile Computing*, vol. 7, no. 5, pp. 647–660, May 2008.

[5] X. Wei, N. Palleit, and T. Weber, "AOD/AOA/TOA-based 3D Positioning in NLOS Multipath Environments," in *Proc. 22nd IEEE Int. Symposium on Personal, Indoor and Mobile Radio Communications (PIMRC'11)*, Toronto, Canada, Sept. 2011, pp. 1294–1298.

[6] B. Y. Shikur and T. Weber, "Posterior CRLB for tracking a mobile station in NLOS multipath environments," in *Proc. IEEE International Conference on Acoustics Speech and Signal Processing (ICASSP'13)*, Vancouver, May 2013, pp. 5175–5179.

[7] J. A. Fessler and A. O. Hero, "Space-alternating generalized expectation-maximization algorithm," *IEEE Transactions on Signal Processing*, vol. 42, no. 10, pp. 2664–2677, Oct. 1994.

[8] J. Li, J. Conan, and S. Pierre, "Mobile terminal location for MIMO communication systems," *IEEE Transactions on Antennas and Propagation*, vol. 55, no. 8, pp. 2417–2420, Aug. 2007.

[9] W. Jakes, *Microwave Mobile Communications*, Wiley-IEEE Press, 1974.

[10] J. C. Liberti and T. S. Rappaport, *Smart Antennas for Wireless Communications: IS-95 and Third Generation CDMA Applications*, Prentice Hall, Upper Saddle River, 1999.

[11] P. Stoica and A. Nehorai, "MUSIC, maximum likelihood, and Cramer-Rao bound," *IEEE Transactions on Acoustics, Speech and Signal Processing*, vol. 37, no. 5, pp. 720–741, 1989.

[12] D. J. Torrieri, "Statistical theory of passive location systems," *IEEE Transactions on Aerospace and Electronic Systems*, vol. 20, no. 2, pp. 183–198, Mar. 1984.

[13] S. M. Kay, *Fundamentals of Statistical Signal Processing: Estimation Theory*, Prentice Hall, Upper Saddle River, 1993.